Development of Tendon-Driven Robot Leg Displaying Gait Motion

Ashwath Karthikeyan[1]
Student, Department of Mechatronics Engineering, SRM Institute of Science and Technology, Kattankulathur
Email : ak7694@srmist.edu.in

Ami Jain[2]
Student, Department of Mechatronics Engineering, SRM Institute of Science and Technology, Kattankulathur
Email : aj4815@srmist.edu.in

Pranav Hanumanthu[3]
Student, Department of Mechatronics Engineering, SRM Institute of Science and Technology, Kattankulathur
Email : ph7419@srmist.edu.in

Ranjith Pillai[4]
Assistant Professor, Department of Mechatronics Engineering, SRM Institute of Science and Technology, Kattankulathur
Email : ranjithr1@srmist.edu.in

Abstract:

In recent years, legged robots have gained significant attention in the field of robotics due to their potential applications in industries such as search and rescue, last-mile delivery, and military operations. These robots excel at navigating challenging terrains where their wheeled counterparts face limitations. Achieving efficient and smooth movement is a crucial aspect for legged robots, with locomotion types like hopping and trotting playing a vital role. Precise control of leg joints is essential to ensure stable and efficient motion. This paper presents a lightweight robot leg prototype with two degrees of freedom that accurately mimics animal leg movement during hopping and trotting. Experimental testing was conducted in lab using a specially designed test rig, which would evaluate the prototype's performance across different ground conditions, facilitating design and control optimization. The modularity of the robot leg prototype allows for easy component replacement and modification. The paper also emphasizes the significance of a robust control system capable of adapting to diverse terrains and effectively handling unexpected disturbances. The paper concludes with the design of the leg prototype with sufficient sensors on board and the test rig for the leg prototype in order to test the control algorithms.

Key words : Robot Leg, Gait Analysis, Trajectory Planning, Tendon-Driven, Legged Robotics

I. INTRODUCTION

Robotics engineers have long been fascinated by the idea of replicating the locomotion abilities of animals in legged mobile robots. However, developing efficient robotic systems that can navigate various terrains remains a challenge. To address this, many researchers are exploring a new approach inspired by animal anatomy, utilizing a tendon mechanism to actuate joints positioned away from the motor [1]-[4].

The focus of this paper is a single-legged robot capable of demonstrating both hopping and trotting gaits. The use of high-torque, back-drivable motors enables the absorption of shock and provides the flexibility to adjust compliance [5]. The addition of elasticity in the tendon mechanism enhances the robot's adaptability to different surfaces [6]. Through this experimental setup, the project aims to optimize the design for maximum power efficiency in achieving hopping and trotting motions.

Fig. 1 illustrates the division of the robot's body into left and right portions along the sagittal plane, which runs longitudinally through the body. The median sagittal plane closely follows the body's midline and equally divides it. Perpendicular to the sagittal plane is the coronal plane, another vertical plane running longitudinally through the body. A horizontal plane, parallel to the ground and perpendicular to both the sagittal and coronal planes, divides the body into upper (superior) and lower (inferior) halves [7].

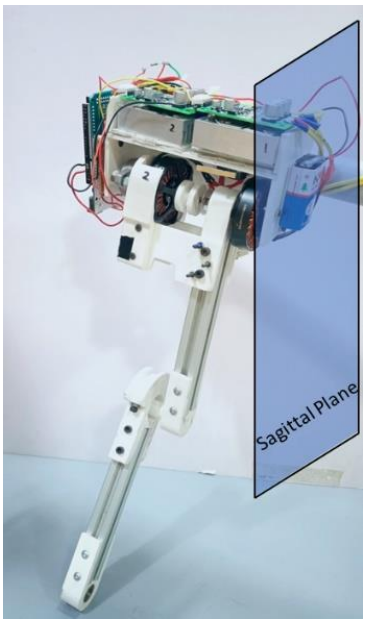

Fig. 1 *Sagittal Plane*

While conventional legged mobile robots typically utilize multiple legs for dynamic balance, this paper focuses on examining the gait and control of a single-legged robot to gain insights into the underlying mechanics. By showcasing the robot's ability to hop and trot, the paper provides a glimpse into the future of robotics, where animal-inspired technology merges with innovative engineering to create robots capable of efficiently navigating and operating in challenging environments.

II. MATHEMATICAL MODELLING AND SIMULATION

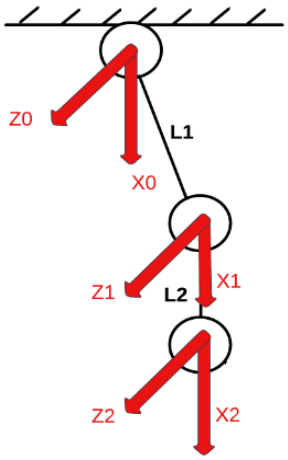

Fig. 2 *Frame assignment of the robot*

The robot leg is modeled as a 2R planar mechanism, a serial manipulator with two rotational joints and an end effector. The hip joint and knee joint are confined to the sagittal plane, simplifying the mathematical equations for defining the robot.

Forward kinematics involves determining the position and velocity of the ankle, acting as the end effector, based on the known joint angles and angular velocities. The link lengths are represented by L_1 and L_2, and the joint axes are assigned as shown in Fig. 2. The angle between X_0 and L_1 is θ_0, and the angle between X_1 and L_2 is θ_1.

A commonly used convention for selecting frames of reference in robotic applications is the Denavit-Hartenberg, or D-H convention. The four quantities θ, a, d, α are parameters associated with link and joint. The four parameters are generally given the names link length, link twist, link offset, and joint angle, respectively. Fig. 2 shows the frame assignment for the leg as per standard D-H convention.

Here, values of D-H parameters of transition between the joints 0,1 and 1,2 are present in the corresponding cross-section point as given in Table 1.

Table 1
D-H Parameters

	θ	d	a	α
0-1	0	0	L1	0
1-2	1	0	L2	0

Once the D-H parameter table has been filled for the robot leg, the homogeneous transformation matrix is found by plugging the values into the matrix of the following form, which is the homogeneous transformation matrix for joint n (i.e. the transformation from frame n-1 to frame n) [8].

Homogeneous Transformation Matrix:

$$\begin{bmatrix} \cos\theta_n & -\sin\theta_n \cos\alpha_n & \sin\theta_n \sin\alpha_n & r_n \cos\theta_n \\ \sin\theta_n & \cos\theta_n \cos\alpha_n & -\cos\theta_n \sin\alpha_n & r_n \sin\theta_n \\ 0 & \sin\theta_n & \cos\alpha_n & d_n \\ 0 & 0 & 0 & 1 \end{bmatrix} \quad (1)$$

The link transformation matrices are as follows:

Transformation matrix of knee joint w.r.t hip joint =

$$\begin{bmatrix} \cos\theta_0 & -\sin\theta_0 & 0 & L_1 \\ \sin\theta_0 & \cos\theta_0 & 0 & 0 \\ 0 & 0 & 1 & 0 \\ 0 & 0 & 0 & 1 \end{bmatrix} \quad (2)$$

Transformation matrix of ankle joint w.r.t knee joint =

$$\begin{bmatrix} \cos\theta_1 & -\sin\theta_1 & 0 & L_2 \\ \sin\theta_1 & \cos\theta_1 & 0 & 0 \\ 0 & 0 & 1 & 0 \\ 0 & 0 & 0 & 1 \end{bmatrix} \quad (3)$$

The forward kinematics of the robot leg can be expressed as

Transformation of end effector w.r.t hip joint =

$$\begin{bmatrix} c_0c_1\text{-}s_0s_1 & -c_0s_1\text{-}\ s_0c_1\text{-} & 0 & L_1c_0+L_2(c_0c_1\text{-}\ s_0s_1) \\ s_0c_1\text{-}c_0s_1 & s_0s_1+\ c_0c_1 & 0 & L_1s_0+L_2(s_0c_1\text{-}\ c_0s_1) \\ 0 & 0 & 1 & 0 \\ 0 & 0 & 0 & 1 \end{bmatrix} \quad (4)$$

Here, $c_0 = \cos\theta_0$, $s_0 = \sin\theta_0$, $c_1 = \cos\theta_1$, $s_1 = \sin\theta_1$
L_1=198mm, L_2=165mm

While forward kinematics helps find the coordinates of the end effector of the robot leg for given joint angles, inverse kinematics is required to find the joint angles required to achieve a desired end effector position and orientation.

Once the inverse kinematics equations are known, they can be used to solve the corresponding joint angles of the desired position and orientation of the end effector.

Subsequently, these joint angles are used to plan a trajectory for the robot leg. Trajectory planning involves determining a sequence of joint angles that the robot needs to follow to smoothly reach the desired end effector position and orientation and perform the required gait motion [9]. The trajectory is parameterized by time.

For a given coordinate of end effector being (x,y), the joint angles θ_0 and θ_1 can be found from equations (5) and (6)

$$x = L_1.\cos\theta_0 + L_2(\cos\theta_0.\cos\theta_1 - \sin\theta_0.\sin\theta_1) \quad (5)$$

$$y = L_1.\sin\theta_0 + L_2(\sin\theta_0 - \cos\theta_1 + \cos\theta_0.\sin\theta_1) \quad (6)$$

The joint angles for the hip joint and knee joint are given in equations (7) and (8)

$$\theta_1 = \pm \cos^{-1}[(x^2 + y^2 - L_1^2 - L_2^2) / 2\, L_1 . L_2)] \quad (7)$$

$$\theta_0 = \tan^{-1}[(y/x) - (L_2.\sin\theta_1 / L_1 + L_2.\cos\theta_1)] \quad (8)$$

By using the inverse kinematics equations and trajectory planning techniques, the joint angles can be computed and a planned trajectory can be generated for the robotic leg to follow, allowing it to accurately reach and move between desired positions and orientations.

III. SIMULATION

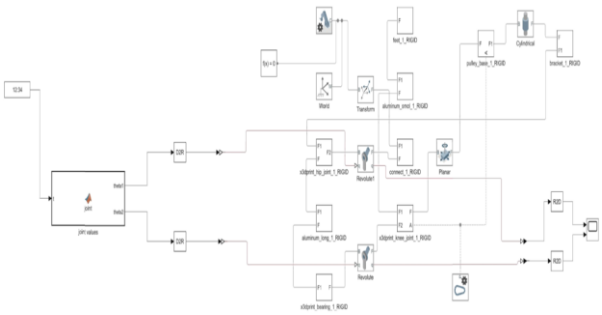

Fig. 3 *Simulink model on MATLAB*

The model design in Fig. 3 helped simulate the motion of the joints in the MATLAB-Simulink environment by using the inbuilt blocks such as the spool system and pulley-belt mechanism to make sure that the mechanical design is efficient before proceeding with the prototyping. It was also used to identify at what distance the motor must be placed from the joint for maximum energy transmission required to achieve the optimal gait motion, and a rough code for the sequence of actuation of the joints with respect to time was formulated. Fig. 4 shows the progression of the simulation of leg motion at different angles.

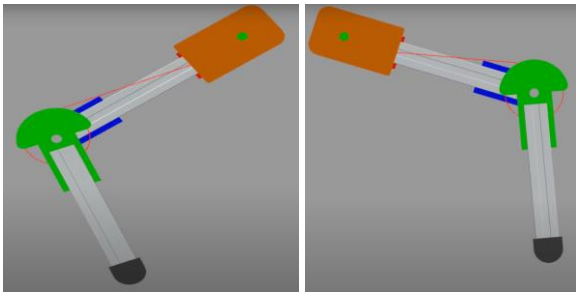

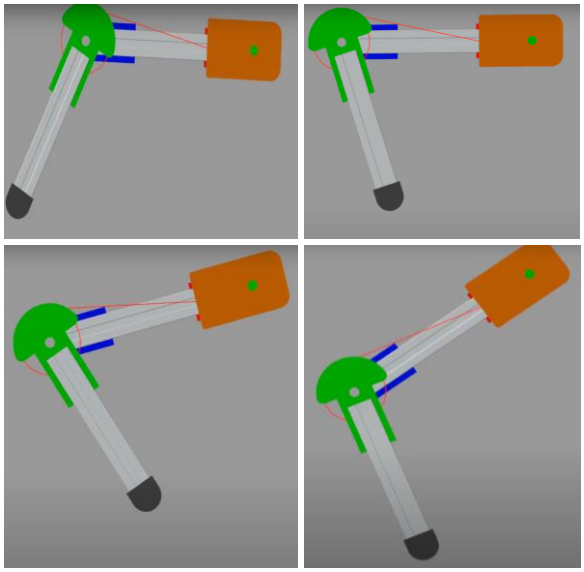

Fig. 4 *Simulation of the progression of leg motion*

IV. MECHANICAL DESCRIPTION

After carefully weighing the pros and cons of several designs, the mechanical setup was put into place so as not to obstruct the leg's ability to perform the hopping activity, and to ensure efficient spacing and ease of troubleshooting. Because the motors are co-axial, as can be seen in Fig. 5, the overall torque and moment of inertia are reduced [10]. A leg's design must strike a balance between many important features, such as low weight, low inertia, high power output, and minimal mechanical complexity. By taking cues from how animals move and using biomechanical concepts, a bioinspired approach to leg design can assist in achieving these objectives.

Tendons were used to distally actuate the knee joint meaning that the transmission takes place through the tendon and the motor controls it while not being located in proximity. By attaching the tendons to the appropriate points on the leg and knee structure, the desired motion and range of movement can be achieved, allowing for precise and controlled flexion and extension of the knee joint.

The use of motors is another crucial factor in leg design. Brushless DC (BLDC) motors in particular are frequently employed because of their effectiveness and high-power output [11]. To prevent imbalance or performance inefficiencies, it is crucial to make sure the motor's weight is spread uniformly across the leg.

The compactness of the assembly, which is one of the robot leg's primary design elements, is made possible by placing the hip joint coaxially with the knee joint. By doing so, this design not only makes the leg appear smaller overall but also increases the hip motor's effectiveness [12].

Furthermore, the coaxial arrangement of the two motors used in the design lowers the moment of inertia and, as a result, the torque needed by the hip motor to lift the assembly. Additionally, the overall stability of the leg during hopping and trotting movements is enhanced by this design.

The lightweight aluminum extrusion used to build the leg framework ensures rigidity while also reducing weight. Additionally, by using PLA-based 3D-printed joints, with a sufficiently high infill ratio, durability is attained. By selecting PLA for the connectors, it was possible to keep a low overall weight while ensuring that the joints could withstand any stresses applied to them during use. Overall, a leg structure that is both strong and lightweight is produced by this mix of building materials and methods.

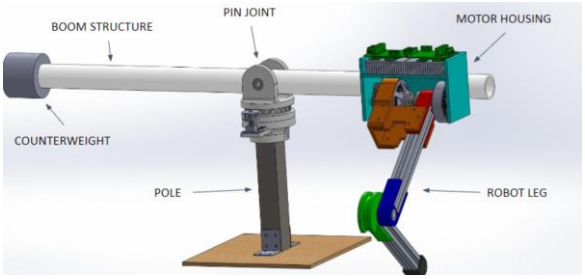

Fig. 5 *Model of the leg and test rig in CAD*

The lightweight 3D printed components utilized in the leg design make it simpler to build the entire leg because they make printing complex sections easier. When the link moves, the knee motor will also move, ensuring precise control of the leg movement. The bracket that holds the knee motor is designed to help attach the knee motor to the link.

The robot leg's design is carefully thought out and tuned to deliver the needed performance while reducing the assembly's weight, complexity, and inertia. The weight of the leg is 1022 grams. The utilization of lightweight materials, a compact design, and bio-inspired characteristics like the tendon have produced a limb that performs stable and effective hopping and trotting movements.

A single-legged hopping robot is a novel research field that has attracted interest [13]. An experimental platform was designed to analyze and comprehend its mechanics. This test apparatus measures the robot's state, i.e., whether it is in the leg swing stage or in the heel strike stage, and restricts motion to the sagittal plane for accuracy. This enables precise study of the hopping gait and its correspondence to sagittal plane models.

A boom structure aids in planarizing the leg in the sagittal plane, as shown in Fig. 5, by rotating with respect to the pole, about the vertical axis [14],[15]. This ensures that there is no need for a third angle about the vertical axis, simplifying the analysis.

A rotary encoder measures the boom's rotation around the pole, converting motion into digital signals. The pole is made of PVC composite and 3D-printed components for stability and smooth movement. L-brackets anchor the pole to the base, ensuring stability.

Test rigs such as this aid locomotion studies and development of efficient systems applicable in robotics, prosthetics, and biomechanics.

V. ELECTRICAL / ELECTRONIC DESCRIPTION

BLDC motors are the actuators used in this paper. This choice is attributed to the following reasons:

1. They are more energy efficient since they do not use brushes, resulting in less friction and heat loss, and hence lower power usage.

2. BLDC motors have a longer lifespan since they have less wear and tear over time due to the lack of brushes that need to be replaced. This lowers maintenance costs while increasing reliability.

3. BLDC motors offer higher power-to-weight ratios, which means they can provide more power for their size and weight. As a result, they are appropriate for use in applications such as this project, which have heavy components as such and cannot afford actuators that will add to that existing load.

4. Most importantly, BLDC motors provide the benefit of back-drivability, and thus dynamic and static compliance, which is essential for cases such as this where interaction from the environment is inevitable [16].

The Antigravity MN5008 KV170 BLDC motors, presented in Fig. 6, were chosen for the project because of their high peak current of 15A, which allows them to produce high amounts of power up to 720W. They have a voltage rating of 6-12S and weigh only 128 grams, making them excellent for situations like this, where weight is critical. The velocity constant, or the KV rating of the motors, is 170, suggesting that when given voltage, they can spin at a corresponding speed. This attribute qualifies them for applications requiring quick and precise movement.

Two BLDC motors are used in the robot leg to achieve two degrees of freedom - one for the hip joint and one for the knee joint. The knee joint has a range of motion of 40 to 125 degrees, while the hip joint has a range of 34 to 81 degrees. These ranges were chosen based on the biomechanical features of animal legs seen while hopping and trotting. Each joint can be operated independently by two motors, allowing for more flexibility and range of motion.

The torque required by the hip motor to lift the entire leg is 1.0637 N.m and the torque required by the knee motor is 0.4380 N.m.

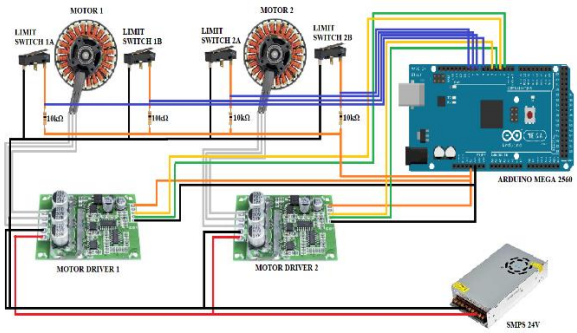

Fig. 6 *Electronic connections*

The Antigravity MN5008 KV170 BLDC motors require a motor driver to control speed and direction using PWM signals. The driver acts as an interface between the microcontroller and motor, regulating current flow based on PWM values. Precise control is crucial, achieved through sensors and software provided by the motor driver. Overloading and overheating protection is also ensured.

The project utilizes the Brushless Motor Controller DC 12-36V 500W PWM Driver board, operating in a 12-36V range with a 1-20 kHz PWM frequency. Two drivers, each handling 15A and 500W, are used for the motors. Lightweight at 30 grams, they provide efficient control while preventing motor damage.

An optical encoder is used as a sensor in this system for precise motor control. It tracks a disk attached to the motor shaft using a light source and a photodetector. The disk has 100 slits or marks, providing accurate position and speed information. The encoder counts the number of times the light passes through a slot, determining the motor's rotation angle.

The encoder has two output ports connected to the Arduino board's GPIO pins, allowing the microcontroller to decode the signals and calculate motor speed for precise control.

Four limit switches are mounted on the leg, two on the knee joint and two on the hip joint. They

notify the controller when a specific position is reached, enabling adjustment of the joint's motion direction. The limit switches ensure maximum joint position is achieved, preventing damage and facilitating calibration.

The Arduino Mega is chosen for its precise control over the motor driver's frequency. Its increased I/O pin count allows for connecting multiple sensors and actuators. PWM, generated by the Arduino's microcontroller or custom PWM controller, enables precise motor speed control. Fig. 6 shows the control circuit diagram used for the speed control of the BLDC motor.

VI. FINAL PROTOTYPE

A robot leg designed for hopping movements is accompanied by an experimental setup. The setup consists of a vertical pole supporting the leg and a horizontal boom restricting its motion to a circular path around the pole. To balance the extended boom's weight, a counterweight is installed on the opposite side. A revolute joint connects the boom and pole, with a potentiometer tracking leg rotations. The leg is a 2R planar mechanism, with each joint actuated by a BLDC motor. The hip joint is directly connected, while the knee joint is actuated using a tendon material. The motors are housed in a box for protection. Fig. 7 shows the final integrated prototype and Fig. 8 displays the robot leg in motion along with the sensors and control circuit on board.

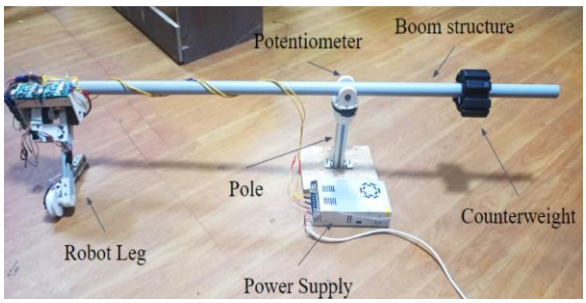

Fig. 7 *Robot Leg with Experimental Setup*

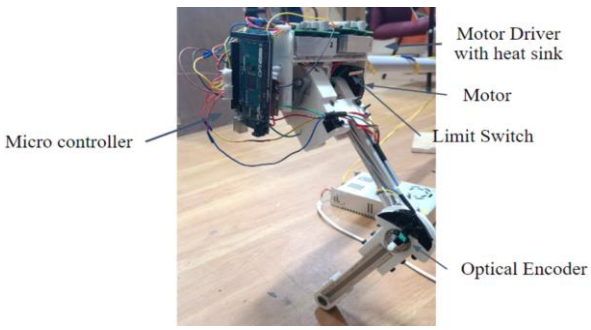

Fig. 8 *Components on the leg*

VII. CONCLUSION

This paper aims to demonstrate the feasibility of tendon-driven actuation for robot legs, showcasing its advantages in scenarios where joint accessibility is limited or actuation needs to be shifted away from the joint itself. The robot leg was fabricated using lightweight 3D-printed material and aluminum, with high tensile strength nylon threads serving as the transmission element. Assembly was optimized for minimal energy loss and other factors. Control of joint motors was accomplished by using microcontrollers such as Arduino, as well as motor drivers. Incorporating springs in the mechanism helped absorb shock during landing. The single-legged robot served as a scalable model for multi-legged robots capable of self-balancing, various gait cycles, and improved energy efficiency, making them suitable for industrial applications with enhanced speed and range of motion.

VIII. REFERENCES

[1] J.P. Whitney, M.F. Glisson, E.L. Brockmeyer, and J.K. Hodgins, "A low-friction passive fluid transmission and fluid-tendon soft actuator," in 2014 IEEE/RSJ International Conference on Intelligent Robots and Systems, pp. 2801-2808, September 2014.

[2] O.B. Farah, Z. Guo, C. Gong, C. Zhu, and H. Yu, "Power analysis of a series elastic actuator for ankle joint gait rehabilitation," in 2015 IEEE International Conference on Robotics and Automation (ICRA), pp. 2754-2760, May 2015.

[3] Q. Tu, Y. Wang, D. Yue, and F.A. Dwomoh, "Analysis on the impact factors for the pulling force of the McKibben pneumatic artificial muscle by a FEM model," Journal of Robotics, pp. 1-11, 2020.

[4] S. Kitano, S. Hirose, A. Horigome, and G. Endo, "TITAN-XIII: sprawling-type quadruped robot with ability of fast and energy-efficient walking," Robomech Journal, vol. 3, pp. 1-16, 2016.

[5] P.M. Wensing, A. Wang, S. Seok, D. Otten, J. Lang, and S. Kim, "Proprioceptive actuator design in the mit cheetah: Impact mitigation and high-bandwidth physical interaction for dynamic legged robots," IEEE Transactions on Robotics, vol. 33, no. 3, pp. 509-522, 2017.

[6] A.T. Spröwitz, M. Ajallooeian, A. Tuleu, and A.J. Ijspeert, "Kinematic primitives for walking and trotting gaits of a quadruped robot with compliant legs," Frontiers in Computational Neuroscience, vol. 8, p. 27, 2014.

[7] M.A. Gaudiani, B.U. Nwachukwu, J.V. Baviskar, M. Sharma, and A.S. Ranawat, "Optimization of sagittal and coronal planes with robotic-assisted unicompartmental knee arthroplasty," The Knee, vol. 24, no. 4, pp. 837-843, 2017.

[8] K.M. Lynch and F.C. Park, "Modern robotics," Cambridge University Press, 2017.

[9] D. Tian, J. Gao, X. Shi, Y. Lu, and C. Liu, "Vertical jumping for legged robot based on quadratic programming," Sensors, vol. 21, no. 11, p. 3679, 2021.

[10] Y. Ding and H.W. Park, "Design and experimental implementation of a quasi-direct-drive leg for optimized jumping," in 2017 IEEE/RSJ International Conference on Intelligent Robots and Systems (IROS), pp. 300-305, September 2017.

[11] F. Grimminger, A. Meduri, M. Khadiv, J. Viereck, M. Wüthrich, M. Naveau, V. Berenz, S. Heim, F. Widmaier, T. Flayols, and J. Fiene, "An open torque-controlled modular robot architecture for legged locomotion research," IEEE Robotics and Automation Letters, vol. 5, no. 2, pp. 3650-3657, 2020.

[12] J. Su, B. Jin, S. Ye, L. Ruan, C. Sun, N. Ding, Y. Fu, and J. Luo, "Maximize the Foot Clearance for a Hopping Robotic Leg Considering Motor Saturation," arXiv preprint arXiv:2107.13717, 2021.

[13] J. Ramos, Y. Ding, Y.W. Sim, K. Murphy, and D. Block, "Hoppy: An open-source kit for education with dynamic legged robots," in 2021 IEEE/RSJ International Conference on Intelligent Robots and Systems (IROS), pp. 4312-4318, September 2021.

[14] M. Bolignari, A. Mo, M. Fontana, and A. Badri-Spröwitz, "Diaphragm Ankle Actuation for Efficient Series Elastic Legged Robot Hopping," in 2022 IEEE/RSJ International Conference on Intelligent Robots and Systems (IROS), pp. 4279-4286, October 2022.

[15] F. Ruppert and A. Badri-Spröwitz, "Series elastic behavior of biarticular muscle-tendon structure in a robotic leg," Frontiers in Neurorobotics, vol. 13, p. 64, 2019.

[16] A. Mazumdar, S.J. Spencer, C. Hobart, J. Salton, M. Quigley, T. Wu, S. Bertrand, J. Pratt, and S.P. Buerger, "Parallel elastic elements improve energy efficiency on the STEPPR bipedal walking robot," IEEE/ASME Transactions on Mechatronics, vol. 22, no. 2, pp. 898-908, 2016.

★★★